

<sup>12</sup>T. A. Brody and M. Moshinsky, *Tables of Transformation Brackets for Nuclear Shell-Model Calculations* (Dirección General de Publicaciones, Universidad Nacional de México, Ciudad Universitaria, Mexico, D. F., 1960).

<sup>13</sup>T. Ueda and A. E. S. Green, Nucl. Phys. **B10**, 289 (1969).

<sup>14</sup>C. W. Lee and E. Baranger, Nucl. Phys. **79**, 385 (1966).

<sup>15</sup>B. H. J. McKellar, Phys. Rev. **134**, B1190 (1964).

<sup>16</sup>P. S. Ganas and B. H. J. McKellar, Phys. Rev. **175**, 1409 (1968).

<sup>17</sup>P. S. Ganas and B. H. J. McKellar, Nucl. Phys. **A120**, 545 (1968).

<sup>18</sup>P. S. Ganas and B. H. J. McKellar, Phys. Rev. **180**, 953 (1969).

<sup>19</sup>J. F. Dawson, I. Talmi, and J. D. Walecka, Ann. Phys. (N. Y.) **18**, 339 (1962).

<sup>20</sup>T. T. S. Kuo and G. E. Brown, Nucl. Phys. **85**, 40 (1966).

<sup>21</sup>R. A. Arndt, R. Bryan, and M. H. MacGregor, Phys. Letters **21**, 314 (1966).

<sup>22</sup>The author thanks Professor Bryan for this remark.

## Magnetic Hyperfine Structure of Muonic Atoms\*

John Johnson† and Raymond A. Sorensen

Carnegie-Mellon University, Pittsburgh, Pennsylvania 15213

(Received 22 January 1970)

Magnetic hyperfine structure in muonic x rays is calculated for several models of the nuclear magnetism and compared to experimental values for <sup>115</sup>In, <sup>127</sup>I, <sup>133</sup>Cs, <sup>139</sup>La, <sup>141</sup>Pr, <sup>151</sup>Eu, <sup>203</sup>Tl, <sup>205</sup>Tl, and <sup>209</sup>Bi. The results are excellent for the realistic models in most cases, and all but one of the nine cases agree within better than two standard deviations with the experiments. For the realistic models, the hyperfine energy is substantially reduced (by about 30% in most cases) from its point-nucleus value. In these models, the single-particle magnetism distribution is modified by the addition of configurations resulting from various residual nuclear interactions, the interaction strength being adjusted in each case to produce the experimental value for the magnetic moment.

### I. INTRODUCTION

The hyperfine splitting of levels in electronic and muonic atoms is due to the interaction of the nuclear magnetism with the magnetic field of the orbiting electron or muon. The energy of interaction depends on the relative orientation of the nuclear magnetism and the field. For a point dipole of strength  $\vec{\mu}$  in a field  $B$  the energy is

$$W = -\vec{\mu} \cdot \vec{B}. \quad (1)$$

Two isotopes have a nearly identical electronic structure, and therefore the magnetic field at the nucleus is the same for each isotope. The hyperfine splitting will be different for the two isotopes because the nuclear moments are different. However, the ratio of the nuclear moments should equal the ratio of the splittings if the nucleus is a point dipole.

In 1947 Bitter<sup>1</sup> made a very accurate measurement of the ratio of the magnetic moments of two rubidium isotopes using magnetic-resonance techniques. This ratio differed slightly from the ratio of the hyperfine structure splittings, indicating Eq. (1) is incorrect. Bitter<sup>2</sup> suggested that the discrepancy was due to an extended distribution of

nuclear magnetism. Bohr and Weisskopf<sup>3</sup> made the first detailed calculations of this "hyperfine anomaly" in 1950, and the effect is sometimes called the "Bohr-Weisskopf" effect. Since then, many more hyperfine anomalies have been measured, making possible a systematic investigation of the effect.<sup>4</sup>

More recently, the hyperfine structure of muonic atoms has been measured for several cases.<sup>5-9</sup> A muonic atom is formed by stopping negatively charged muons in a target. The muon is captured by an atom and makes Auger and radiative (x-ray) transitions down through the atomic orbits until it reaches the 1s state. It is then either captured by the nucleus via the weak interaction, or it decays. Since the muon is 206 times heavier than an electron, its orbits are 206 times closer to the nucleus than the equivalent electron orbits. The muon energy levels are thus quite sensitive to the nuclear structure. By observing the x rays given off in the transitions, one can learn something about nuclear structure. In particular, the hyperfine structure of the x rays depends on the distribution of magnetism of the nucleus and differs from that calculated for a point nucleus by as much as 50%.

The hyperfine structure in muonic atoms is usually observed as a broadening of the x ray given

off by the atom when the muon makes a transition. The experimental resolution is good enough so that it is possible to make fits to the broadening by folding in the hyperfine components with the correct intensities and line shape. In  $^{203}\text{Tl}$  and  $^{205}\text{Tl}$  the nucleus can be excited in the muon-cascade process.<sup>9</sup> The lifetime of this state is such that the muon reaches the 1s state before the nucleus deexcites to the ground state. The  $\gamma$  ray of the nuclear decay is given off with the muon in the 1s state and it is found to be split into two components due to the hyperfine structure of the nucleus-muon system. This splitting is well resolved by solid-state detectors, because of the good absolute resolution at the energies of the nuclear  $\gamma$  ray ( $\sim 200$  keV).

LeBellac<sup>10</sup> first calculated the effect in muonic atoms for a few cases. These measurements of muonic hyperfine spectra can be used to distinguish between nuclear models which are approximately equivalent in other respects, and lead to greater understanding of nuclear structure.

## II. HYPERFINE INTERACTION ENERGY

Since the nucleus is not a point dipole magnet, we must integrate over the volume of magnetization to find the energy in a magnetic field:

$$W = - \int \vec{M}(\vec{R}) \cdot \vec{B}(\vec{R}) d^3R. \quad (2)$$

Bohr and Weisskopf<sup>3</sup> calculated this hyperfine interaction energy using relativistic perturbation theory for an electron or muon in an  $s_{1/2}$  or  $p_{1/2}$  state. The total energy due to magnetic hyperfine interactions is given by

$$\begin{aligned} W &= A[F(F+1) - I(I+1) - J(J+1)] / (2IJ), \\ A &= - \frac{2eK\mu_N}{J+1} \sum_{i=1}^A \int d^3R \psi^*(\vec{R}) [(g_i L_{z_i} + g_{s_i} S_{z_i}) \\ &\quad \times \int_{R_i}^{\infty} f(r)g(r)dr + (g_i L_{z_i} + g_{s_i} \hat{a}_{z_i}) R_i^{-3} \\ &\quad \times \int_0^{R_i} f(r)g(r)r^3 dr] \psi(\vec{R}), \end{aligned} \quad (3)$$

where  $r$  is the electron or muon radial coordinant,  $\vec{R}$  represents the nuclear coordinants including spin,  $\psi$  is the nuclear wave function,  $f$  and  $g$  are the Dirac radial wave functions, and  $J$  is the angular momentum of the electron or muon.  $I$  is the nuclear angular momentum,  $F$  is the total angular momentum,  $L_{z_i}$  and  $S_{z_i}$  are the nucleon-orbital and spin-angular-momentum operators,  $g_i$  and  $g_{s_i}$  are the nucleon orbital and spin gyromagnetic ratios,

$\mu_N$  is the nuclear magneton, and

$$K = \mp(J + \frac{1}{2}) \quad \text{for } J = I \pm \frac{1}{2} \quad (4)$$

and

$$\hat{a} = -\sqrt{2\pi}(S \otimes Y_2)^1, \quad (5)$$

where the nucleon spin  $S$  and rank-2 spherical harmonic are coupled to form a rank-1 tensor.

The relativistic muon wave functions  $f(r)$  and  $g(r)$  are calculated by numerical integration of the Dirac equation using the Fermi form for the nuclear charge distribution which gives the best fit to the  $K$  and  $L$  muonic x-ray energies. Then Eq. (3) is used to calculate the hyperfine splitting for the various nuclear wave functions.

## III. NUCLEAR MODELS

Most of the nuclear models used in this work have previously been used to calculate nuclear magnetic moments. Here we extend the application of the models by calculating hyperfine structure. In this way we hope to differentiate between models which give the same moment.

### A. Single-Particle Model

The single-particle or Schmidt model, assumes the magnetism is due entirely to the last odd particle in the shell model. This particle is usually assumed to have its free-particle spin gyromagnetic ratio of 5.5858 and  $-3.826\mu_N$  for protons and neutrons, respectively. In general this model does not do well in predicting magnetic moments, but provides a good zeroth-order approximation for other models. The contribution of a single nucleon is obtained from Eq. (3) with a single-particle nuclear wave function. The result is<sup>10</sup>

$$\begin{aligned} A &= - \frac{2eK\mu_N}{J+1} \left\{ \left[ \frac{1}{2}g_s + (I + \frac{1}{2})g_i \right] K_a \right. \\ &\quad \left. + \left[ - \frac{2I-1}{8(I+1)}g_s + (I - \frac{1}{2})g_i \right] K_b \right\}, \quad \text{for } I = I + \frac{1}{2}, \\ A &= - \frac{2eK\mu_N}{J+1} \left\{ \left[ - \frac{g_s}{2(I+1)} + \frac{2I+3}{2(I+1)}g_i \right] IK_a \right. \\ &\quad \left. + \left[ \frac{2I+3}{8I(I+1)}g_s + \frac{2I+3}{2(I+1)}g_i \right] IK_b \right\}, \quad \text{for } I = I - \frac{1}{2}, \end{aligned} \quad (6)$$

$$K_a \equiv \int_0^{\infty} R_{n_i}^2(R)R^2 dR \int_R^{\infty} f(r)g(r)dr, \quad (6a)$$

$$K_b \equiv \int_0^{\infty} R_{n_i}^2(R)R^{-1} dR \int_0^R f(r)g(r)r^3 dr. \quad (6b)$$

### B. Configuration-Mixing Models

Arima and Horie<sup>11</sup> and Blin-Stoyle<sup>12</sup> proposed a model which introduces configuration-mixing corrections to the Schmidt model. They assume the magnetism is due to the last odd particle plus particle-hole excited states which are admixed into the ground state of the system by a short-range residual interaction. In perturbation theory the unnormalized ground-state wave function becomes

$$|\psi\rangle = |\psi_0\rangle + \sum_i \frac{\langle \psi_i | V | \psi_0 \rangle}{E_0 - E_i} |\psi_i\rangle, \quad (7)$$

where  $|\psi_0\rangle$  is the unperturbed ground state,  $|\psi_i\rangle$  are particle-hole excited states, and  $E_0$  and  $E_i$  are the respective unperturbed energies. The expectation value of any operator  $F$  in lowest order is

$$\langle \psi | F | \psi \rangle = \langle \psi_0 | F | \psi_0 \rangle + 2 \operatorname{Re} \sum_i \alpha_i \langle \psi_0 | F | \psi_i \rangle, \quad (8)$$

$$\alpha_i = \langle \psi_i | V | \psi_0 \rangle / (E_0 - E_i). \quad (9)$$

If  $F$  is the magnetic-moment operator, the first term is just the single-particle moment and the second term is the correction. The off-diagonal matrix elements of  $\mu$  can be large compared to the Schmidt moment. In such cases small admixtures can give substantial contributions to the moment.

We may also calculate contributions of these particle-hole excited states to the hyperfine structure. In this case the operator  $F$  in Eq. (8) is the hyperfine-structure operator whose expectation value is given in Eq. (3). The first term of Eq. (3) is similar to the moment expectation value. The correction to the single-particle contribution for the first term is then the same as the correction to the single-particle moment except for the radial integrals. The second term is also very simple. It can be shown that for  $\Delta l = 0$  transitions

$$\langle j \| \hat{a} \| j' \rangle = \frac{1}{4} \langle j \| \vec{S} \| j' \rangle. \quad (10)$$

Thus the second term of Eq. (3) gives a correction to the hyperfine structure which, except for the radial integrals, is the same as the moment correction with  $g_s$  replaced by  $\frac{1}{4}g_s$ . The correction for the  $\Delta l = 0$  mixing terms is

$$\begin{aligned} \delta A_i = & -\frac{2eK\mu_N}{J+1} \delta\mu_i \left[ \int_0^\infty R_{n_1 j}(R) R_{n_1 j'}(R) R^2 dR \int_R^\infty f g d r \right. \\ & \left. + \frac{\frac{1}{4}g_s - g_l}{g_s - g_l} \int_0^\infty R_{n_1 j}(R) R_{n_1 j'}(R) R^{-1} dR \int_0^R f g r^3 d r \right], \end{aligned} \quad (11)$$

where  $\delta\mu_i$  is the correction to the magnetic moment due to a particle-hole admixed pair with orbital angular momentum  $l$ .

The  $\hat{a}$  operator also connects states which differ in orbital angular momentum by 2. We find this correction to be about two orders of magnitude smaller than the other corrections.

### C. BCS Models

We may also use BCS<sup>13</sup> theory to treat the short-range interaction on a more fundamental basis. The simple pairing force gives no correction to the magnetism. However, the complete  $\delta$  force may be treated in perturbation theory as an interaction between the quasiparticles. The resulting three-quasiparticle admixtures to the one-quasiparticle ground state of an odd nucleus give corrections which are analogous to the particle-hole admixtures used by Arima and Horie. The corrections differ from those derived by Noya, Arima, and Horie.<sup>14</sup> For example, in the Type-I correction [Eq. (4.11) of Ref. 14] the factor involving the particle numbers  $n_c$ ,  $n_b$ , which represents the probability of the fullness of state  $c$  times the probability of the emptiness of state  $b$ , becomes the  $U, V$  factor in the quasiparticle representation:

$$\begin{aligned} & \frac{n_c(2j_b+1-n_b)}{(2j_c+1)(2j_b+1)} - (U_b V_c - U_c V_b)^2 \\ & = (U_b V_c)^2 - 2U_b V_c U_c V_b + (U_c V_b)^2. \end{aligned} \quad (12)$$

The quasiparticle factor is the same for the other types of corrections. The first term of this factor,  $U_b^2 V_c^2$ , is just the probability of the fullness of  $c$  times the probability of the emptiness of states  $b$ . The third term  $U_c^2 V_b^2$  is the opposite of the first term and allows contributions from downward-jumping particles, schematically represented in Fig. 1.

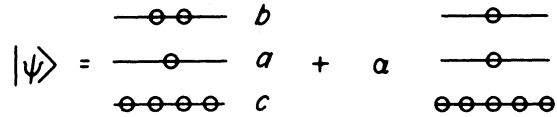


FIG. 1. Schematic representation of  $U_c^2 V_b^2$ .

The cross term will be interpreted after the discussion of the projection method below.

The BCS calculations were carried out only over valence particles. However, there are important contributions from transitions between spin-orbit partners which cross shell boundaries. For example, the  $1g_{9/2}$  level is in the shell below magic number 50, and the  $1g_{7/2}$  level is above. In these

cases a level below the shell in consideration was taken to be full:  $U=0$  and  $V=1$ . A level above the shell in consideration was taken to be empty:  $V=0$  and  $U=1$ .

Another approach used by Kisslinger and Freed<sup>15</sup> is to project out the component of the BCS wave function which has the correct number of particles, and to treat the  $\delta$ -function interaction in perturbation theory using the projected wave functions:

$$|\psi\rangle = |\psi_{\text{even}}\rangle + |\psi_{\text{odd}}\rangle,$$

$$|\psi_{\text{even}}\rangle = \sum_{n_1+n_2+\dots+n_e=n_e} a_{n_1 n_2 \dots}^{(e)} |j_1^{n_1}(0) j_2^{n_2}(0) \dots\rangle, \quad (13)$$

$$|\psi_{\text{odd}}\rangle = \sum_{n_1+n_2+\dots+p=n_o} a_{n_1 n_2 \dots p}^{(o)} |j_1^{n_1}(0) j_2^{n_2}(0) \dots j^p(j) j m\rangle.$$

$|\psi_{\text{even}}\rangle$  is the wave function for the nucleon type (neutrons or protons) with an even number of particles and  $|\psi_{\text{odd}}\rangle$  is the wave function for the type with an odd number of particles.  $n_i$  is the number of particles in the  $i$ th state, and  $p$  is the number of particles in the state of the odd nucleon. This state is a linear combination of all configurations in the valence shell having the correct number of both types of particles. The admixture amplitudes are given by

$$|a_{n_1 n_2 \dots}^{(e)}|^2 = \left[ \sum_{\text{even}} |a^{(e)}|^2 \right]^{-1} \prod_{\text{even}} U_i^{2j_i+1-n_i} V_i^{n_i} \times \frac{(j_i + \frac{1}{2})!}{(\frac{1}{2}n_i)! (j_i + \frac{1}{2} - \frac{1}{2}n_i)!}, \quad (14)$$

$$|a_{n_1 n_2 \dots p}^{(o)}|^2 = \left[ \sum_{\text{odd } i=j} |a^{(o)}|^2 \right]^{-1} \prod_{\text{odd } i=j} U_i^{2j_i+1-n_i} V_i^{n_i} U_j^{2j-p} V_j^{p-1} \times \frac{(j_i + \frac{1}{2})!}{(\frac{1}{2}n_i)! (j_i + \frac{1}{2} - \frac{1}{2}n_i)!} \frac{(j - \frac{1}{2})!}{[(p-1)/2]! (j - \frac{1}{2}p)!}.$$

Kisslinger and Freed take the moment to be

$$\mu = \mu_{\text{sp}} + \sum_{\text{even}} |a_c^{(e)}|^2 \delta\mu_c^{(e)} + \sum_{\text{odd}} |a_c^{(o)}|^2 \delta\mu_c^{(o)}. \quad (15)$$

$\delta\mu_c^{(e)}$  and  $\delta\mu_c^{(o)}$  are calculated exactly the same as in Ref. 14 for each configuration. The sums are over configurations.

Equation (15) does not include any cross terms between different configurations. To see how these terms can contribute, consider six particles to be put in pairs in two levels which are spin-orbit partners. For example consider the levels to be a  $d_{5/2}$  and a  $d_{3/2}$ . The configurations are  $(d_{5/2})^6$ ,  $(d_{5/2})^4(d_{3/2})^2$ , and  $(d_{5/2})^2(d_{3/2})^4$ . The projected wave function will be a linear combination of these three states. The correction to the moment

using this wave function is given by Eq. (15) plus the following cross terms:

$$\langle (d_{5/2})^6 | \mu | (d_{5/2})^5(d_{3/2}) \rangle \langle (d_{5/2})^5(d_{3/2}) | V | (d_{5/2})^4(d_{3/2})^2 \rangle$$

and

$$\langle (d_{5/2})^4(d_{3/2})^2 | \mu | (d_{5/2})^3(d_{3/2})^3 \rangle \times \langle (d_{5/2})^3(d_{3/2})^3 | V | (d_{5/2})^2(d_{3/2})^4 \rangle.$$

Kisslinger and Freed neglect these terms. They are included in the quasiparticle method in the cross term of Eq. (12). We expect these corrections to the projection method to be very small in most cases, since the amplitude for states like  $(d_{5/2})^4(d_{3/2})^2$  and  $(d_{5/2})^2(d_{3/2})^4$  will be small. The only states with large amplitudes will have the upper level of the spin-orbit pair empty or the lower level full.

Equation (11) is used to calculate the hyperfine structure for the quasiparticle and projection models. In general there are more levels contributing to the correction term in these two models than in the simple configuration-mixing model.

#### D. Pairing-Plus-Quadrupole Model

Kisslinger and Sorensen<sup>16</sup> (KS) have investigated the effect of a long-range quadrupole force on the magnetic moments. They diagonalize an interaction between the quasiparticles and phonons which can create or destroy one phonon and scatter the odd quasiparticle. The resulting wave function is a linear combination of one quasiparticle, one quasiparticle coupled to one phonon, and one quasiparticle coupled to two phonons:

$$|\psi_j\rangle = C_{j00}^j \alpha_j^\dagger |\psi_0\rangle + \sum_{j'} C_{j'12}^j (\alpha_{j'}^\dagger \Gamma_2^\dagger)_j |\psi_0\rangle + \sum_{j'J} C_{j'2J}^j [\alpha_{j'}^\dagger (\Gamma_2^\dagger \Gamma_2^\dagger)_J] |\psi_0\rangle. \quad (16)$$

The notation is that of KS:  $C_{j'nJ}^j$  is the amplitude for a quasiparticle of angular momentum  $j'$  coupled to  $n$  phonons with angular momentum  $J$  to make a state of angular momentum  $j$ , and values are tabulated by KS. It is also assumed that the moment operator can be divided into one part operating only on quasiparticles and one operating on phonons:

$$\mu_{\text{op}} \cong \mu_{\text{qp}} + g_R R_z, \quad (17)$$

where  $\vec{R}$  is the phonon angular momentum and  $g_R$  is the phonon gyromagnetic ratio.

The expectation value of this moment for the state given by Eq. (16) is

$$\langle \psi_j | \mu_{op} | \psi_j \rangle = (C_{j00}^j)^2 \mu_{qp}(lj) + \mu_1 + \mu_2, \quad (18)$$

where  $\mu_1$  is the contribution of the one-phonon states and  $\mu_2$  is the contribution of the two-phonon states given by KS.

The contribution of the collective states is small according to KS. The main effect is to change the amplitude of the one-quasiparticle states and mix other one-quasiparticle states into the ground state. The phonons themselves contribute very little, because of their small amplitude in most cases and the small gyromagnetic ratio, which must be of the order of

$$g_R \cong Z/A. \quad (19)$$

In order to get reasonable agreement with the experimental moments it is again necessary to include the  $\delta$ -function force. KS do this in an approximate way by replacing  $\mu_{qp}(lj)$  by the quasiparticle moments calculated by the projection method.

We may also use the quadrupole model to calcu-

$$\begin{aligned} A(lj) = & (C_{j00}^j)^2 A_{qp}(lj) + \sum_{j'} (C_{j'12}^j)^2 \left[ \frac{j'(j'+1) + j(j+1) - 6}{2j'(j+1)} A_{qp}(l'j') + \frac{j(j+1) + 6 - j'(j'+1)}{2(j+1)} A_{\text{phonon}} \right] \\ & + 2 \sum_{i'} C_{i'+\frac{1}{2}12}^j C_{i'-\frac{1}{2}12}^j (g_s - g_i) (U_{i'+\frac{1}{2}} U_{i'-\frac{1}{2}} + V_{i'+\frac{1}{2}} V_{i'-\frac{1}{2}}) \left( -\frac{2eK\mu_N}{J+1} \right) \left( K_a + \frac{\frac{1}{4}g_s - g_e}{g_s - g_e} K_b \right) (g_s - g_i) \quad (22) \\ & \times \frac{[(j+l'+\frac{7}{2})(l'-j+\frac{5}{2})(l'+j-\frac{3}{2})(j-l'+\frac{5}{2})]^{1/2}}{2(2l'+1)(j+1)} - \frac{\frac{3}{4} \sum_{\substack{\Delta l=2 \\ j_2=j_1+1}} C_{j_112}^j C_{j_212}^j (U_{j_1} U_{j_2} + V_{j_1} V_{j_2}) \left( -\frac{2eK\mu_N}{J+1} g_s K_b \right)}{j^2(j+1)} \\ & \times \frac{[(j+j_2+3)(j+j_2-2)(j_2+2-j)(j+3-j_2)]^{1/2}}{j^2(j+1)}. \end{aligned}$$

The form for the radial integrals  $K_a$  and  $K_b$  is given in Eq. (6a, b), except that  $R_n^2$  is replaced by the product of the two radial wave functions of the particle-hole pair.  $A_{qp}(lj)$  is the single-particle contribution corrected by the  $\delta$ -function interaction using the projection method as discussed above.

#### E. Choice of Parameters

We have calculated muonic hyperfine structure and the hyperfine anomaly using the configuration-mixing model of Arima and Horie, the pairing model corrected by a  $\delta$ -function interaction, and the pairing-plus-quadrupole model also corrected by the  $\delta$ -function interaction. Conventional Woods-Saxon wave functions were used to calculate the radial integrals.

The parameters for the pairing calculation were

late hyperfine structure. Here, by analogy with the moment calculation, we separate the contribution of the quasiparticles and the phonon. The phonon contribution is taken to be a surface current with angular momentum 2 and a gyromagnetic ratio of  $g_R$ . The radial wave function of the phonon is:

$$|R_{\text{phonon}}(R)|^2 = \frac{\delta(R - R_0)}{R_0^2}, \quad (20)$$

where  $R_0$  is the nuclear radius.

The phonon contribution to the hyperfine structure is

$$A_{\text{phonon}} = -\frac{2eK\mu_N}{J+1} g_R \left( \int_{R_0}^{\infty} f g dr + R_0^{-3} \int_0^{R_0} f g r^3 dr \right). \quad (21)$$

The quasiparticle contribution is taken to be that corrected by the  $\delta$ -function interaction. Also included are the  $\Delta l = 0, \pm 2$  contributions of the long-range quadrupole force. The hyperfine structure for the wave function given by Eq. (16) is

taken from KS. The strength of the quadrupole force was chosen in each case by fitting the average energy of the 2+ first excited state of the two neighboring even-even nuclei using the random-phase approximation as discussed by KS. For semimagic  $\pm 1$  nuclei, the 2+ energy of the neighboring semimagic nucleus only was fit. Two-phonon admixtures were neglected. The energy denominators were calculated using a single-particle energy given by

$$\begin{aligned} E(nlj) = & [41A^{-1/3} (N + \frac{3}{2}) + 7.0A^{-2/3} (j + \frac{1}{2}) \\ & - 0.02A^{-1/3} l(l+1)] \text{ MeV}, \quad (23) \end{aligned}$$

$$\text{for } j = l \pm \frac{1}{2}, \quad N = 2n + l - 2.$$

In addition to the difference in single-particle energies, a pairing energy  $E_p$  must be added, since

a pair is broken in the hole state. We approximate this energy by

$$E_p = - (j + \frac{1}{2}) 60/A \text{ MeV}, \quad (24)$$

where  $j$  is the angular momentum of the broken pair. For all cases of interest, each particle-hole pair is in the same harmonic-oscillator shell. Only in the small  $\Delta l = 2$  terms does the last term of Eq. (23) enter. Therefore the spin-orbit splitting term is the only important one.

#### IV. RESULTS

The results for muonic hyperfine structure are given in Table I for the single-particle model, a point nucleus, the configuration-mixing model, the pairing model, and the pairing-plus-quadrupole model with a phonon gyromagnetic ratio of 0 and  $Z/A$ , and the quasiparticle moments corrected by the  $\delta$ -function force using the projection method. The results of the quasiparticle method are almost identical to those of the projection method and are therefore not presented here.

Since the hyperfine structure is strongly dependent on the moment, only models yielding the experimental magnetic moment should be compared with experimental results for the hyperfine structure. The moment must be fit in a physically reasonable way. We fit the experimental moment in all realistic models (except the single-particle model which has the Schmidt value for the moment) by varying the singlet strength of the  $\delta$ -function interaction. This calculation is not intended to take into account meson-current effects, but probably gives a good estimate of the distribution of magnetism due to meson effects. We expect these to be associated mainly with the valence particles, since the particles of the core are paired to angular momentum zero. The range of the effects will be small, since the virtual mesons have only a short range compared to the diameter of the nucleus. Therefore the magnetism due to meson effects will be localized around the valence particles. This magnetism may be simulated by configuration mixing, since the mixing involves only valence particles, and since the  $\Delta l = 0$  admixtures mainly change the distribution of spin magnetism of the valence particles.<sup>17</sup>

Magnetic hyperfine structure has been measured in nine muonic atoms. In indium, iodine, cesium, lanthanum, praseodymium, and bismuth the agreement of experiment with the reasonable models is very good. The deviation from a point moment is quite large (14 standard deviations in the case

of Pr<sup>141</sup>). However, except for the single-particle model, which has the wrong moment, and the point nucleus, the models all give similar results, making it impossible to make a judgment among the reasonable models in these cases.

In <sup>151</sup>Eu the agreement is not good. <sup>151</sup>Eu is on the edge of the deformed region. The other stable isotope <sup>153</sup>Eu has a rotational spectrum and a large quadrupole moment. The moment is well predicted by all the models, but this may be just an accident, since the moments of the odd promethium and samarium isotopes,<sup>18</sup> and the hyperfine structure of <sup>151</sup>Eu are poorly fit. The pairing-plus-quadrupole model with a gyromagnetic ratio of  $Z/A$  is worse than the other models. However, the measured gyromagnetic ratios of 2+ states in samarium and gadolinium are 0.25 to 0.4, less than  $Z/A$ .

In the thallium isotopes the agreement is only fair. These isotopes are predicted to have very small phonon amplitudes in the ground state. The single-particle strengths found by transfer-reaction experiments in thallium indicate stronger quadrupole coupling.<sup>19</sup> Covello and Sartoris<sup>20</sup> have made intermediate-coupling calculations for the thallium isotopes which fit the transfer-reaction experimental data very well. They require a large coupling strength between the odd-proton hole and the core vibrations. We have repeated the calculations in thallium with the pairing-plus-quadrupole model using a greater quadrupole force strength which would give rise to a phonon energy of 0.4 MeV in the neighboring lead isotopes. The resulting wave functions are very similar to these obtained by Covello and Sartoris. These wave functions improve the agreement with experiment with a phonon gyromagnetic ratio of 0, but make it worse with a ratio of  $Z/A$ .

Also in Table I are the calculations for some other isotopes which may have measurable magnetic hyperfine structure. We include calculations for the  $\frac{7}{2}+$  excited state in <sup>151</sup>Eu. It may be possible to observe the 22-keV nuclear  $\gamma$  with the muon in the 1s state, since the  $\frac{7}{2}+$  state is excited in the muon cascade.<sup>5</sup>

#### V. CONCLUSION

Muonic hyperfine structure and the hyperfine anomaly can offer new information on nuclear structure. Nuclear models which fit magnetic moments will not necessarily correctly predict hyperfine structure. We have obtained excellent agreement in six of nine measured cases. Although all the models of distributed magnetism which fit the moment give results too similar to be distinguished by the experimental values of the

TABLE I. The magnetic hyperfine structure constant in keV. The upper row for each isotope is for the muon in the  $s_{1/2}$  state and the lower row for a  $p_{1/2}$  muon. Column 1 lists the calculated value for the single-particle model with the Schmidt moment. The other columns (2-6) list the calculated values for models all adjusted to have the experimental moment listed under the isotope identified in the column headings. Models in columns 3-6 include the  $\delta$  interaction.

|  | Single-<br>particle<br>model | Point<br>nucleus | Configuration<br>mixing | Pairing<br>model | Pairing-plus-<br>quadrupole model<br>$g_R=0$ | Pairing-plus-<br>quadrupole model<br>$g_R=Z/A$ | Measured<br>values | Ref. |
|--|------------------------------|------------------|-------------------------|------------------|--|--|--------------------|------|
| $^{93}_{41}\text{Nb } \frac{9}{2}+$                        | 1.63                         | 2.32             | 1.48                    | 1.48             | 1.48   | 1.55   |                    |      |
| $\mu = 6.1671$   | 0.365                        | 0.426            | 0.332                   | 0.331            | 0.331  | 0.347  |                    |      |
| $^{113}_{49}\text{In } \frac{9}{2}+$                       | 1.91                         | 2.61             | 1.58                    | 1.58             | 1.58   | 1.67   |                    |      |
| $\mu = 5.5233$   | 0.556                        | 0.637            | 0.457                   | 0.456            | 0.456  | 0.481  |                    |      |
| $^{115}_{49}\text{In } \frac{9}{2}+$                       | 1.91                         | 2.60             | 1.58                    | 1.58             | 1.57   | 1.66   | $1.65 \pm 0.15$    | a    |
| $\mu = 5.5351$   | 0.555                        | 0.637            | 0.457                   | 0.457            | 0.457  | 0.481  | $0.55 \pm 0.20$    |      |
| $^{121}_{51}\text{Sb } \frac{5}{2}+$                       | 1.44                         | 1.64             | 1.04                    | 1.04             | 1.04   | 1.18   |                    |      |
| $\mu = 3.359$  | 0.436                        | 0.431            | 0.312                   | 0.313            | 0.313  | 0.354  |                    |      |
| $^{123}_{51}\text{Sb } \frac{7}{2}+$                       | 0.847                        | 1.23             | 1.07                    | 1.07             | 1.05   | 1.17   |                    |      |
| $\mu = 2.546$  | 0.226                        | 0.326            | 0.297                   | 0.297            | 0.293  | 0.327  |                    |      |
| $^{127}_{53}\text{Tl } \frac{5}{2}+$                       | 1.47                         | 1.40             | 0.940                   | 0.930            | 0.918  | 1.11   | $0.87 \pm 0.09$    | a    |
| $\mu = 2.8091$   | 0.476                        | 0.399            | 0.296                   | 0.294            | 0.291  | 0.352  | $0.33 \pm 0.08$    |      |
| $^{133}_{55}\text{Cs } \frac{7}{2}+$                       | 0.908                        | 1.34             | 1.21                    | 1.18             | 1.17   | 1.21   | $1.16 \pm 0.17$    | a    |
| $\mu = 2.5789$   | 0.277                        | 0.405            | 0.378                   | 0.369            | 0.367  | 0.380  | $0.55 \pm 0.22$    |      |
| $^{139}_{57}\text{La } \frac{7}{2}+$                       | 0.944                        | 1.50             | 1.29                    | 1.30             | 1.30   | 1.30   | $1.22 \pm 0.15$    | b    |
| $\mu = 2.7781$   | 0.304                        | 0.481            | 0.429                   | 0.431            | 0.431  | 0.432  |                    |      |
| $^{141}_{59}\text{Pr } \frac{5}{2}+$                       | 1.61                         | 2.41             | 1.47                    | 1.47             | 1.47   | 1.48   | $1.52 \pm 0.06$    | c    |
| $\mu = 4.28$   | 0.598                        | 0.811            | 0.541                   | 0.544            | 0.544  | 0.544  |                    |      |
| $^{151}_{63}\text{Eu } \frac{5}{2}+$                       | 1.67                         | 2.04             | 1.23                    | 1.24             | 1.23   | 1.43   | $0.80 \pm 0.27$    | d    |
| $\mu = 3.463$  | 0.680                        | 0.772            | 0.499                   | 0.503            | 0.498  | 0.583  |                    |      |
| $^{151}_{63}\text{Eu } \frac{7}{2}+$                       | 1.02                         | 1.52             | 1.30                    | 1.31             | 1.27   | 1.51   |                    |      |
| $\mu = 2.58$   | 0.389                        | 0.575            | 0.503                   | 0.508            | 0.493  | 0.576  |                    |      |
| $^{203}_{81}\text{Tl } \frac{1}{2}+$                       | 1.16                         | 1.19             | 0.768                   | 0.774            | 0.770  | 0.777  | $0.665 \pm 0.075$  | e    |
| $\mu = 1.61169$  | 0.613                        | 0.631            | 0.407                   | 0.410            | 0.408  | 0.412  |                    |      |
| $^{203}_{81}\text{Tl } \frac{1}{2}+$<br>( $\omega = 0.4$ ) |                              |                  |                         |                  | 0.699  | 0.823  |                    |      |
|  |                              |                  |                         |                  | 0.370  | 0.430  |                    |      |
| $^{205}_{81}\text{Tl } \frac{1}{2}+$                       | 1.15                         | 1.19             | 0.774                   | 0.779            | 0.779  | 0.779  | $0.580 \pm 0.015$  | e    |
| $\mu = 1.62754$  | 0.612                        | 0.635            | 0.411                   | 0.413            | 0.413  | 0.413  |                    |      |
| $^{205}_{81}\text{Tl } \frac{1}{2}+$<br>( $\omega = 0.4$ ) |                              |                  |                         |                  | 0.710  | 0.824  |                    |      |
|  |                              |                  |                         |                  | 0.377  | 0.437  |                    |      |
| $^{209}_{83}\text{Bi } \frac{9}{2}-$                       | 1.64                         | 3.04             | 2.06                    |                  |  |  | $1.92 \pm 0.14$    | f    |
| $\mu = 4.0794$   | 0.893                        | 1.67             | 1.12                    |                  |  |  |                    |      |

<sup>a</sup>Reference 9; report of work prior to publication.

<sup>b</sup>A. C. Thompson, Ph.D. thesis, Carnegie-Mellon University, 1969 (unpublished).

<sup>c</sup>Reference 7.

<sup>d</sup>References 5, 6.

<sup>e</sup>Reference 8.

<sup>f</sup>Reference 6; R. B. Sutton, private communication.

hyperfine structure, this fact does give us confidence that the theoretical description of the distribution of magnetism is quite good for heavy spherical nuclei.

H. H. Stroke has pointed out that a theoretical study of hyperfine structure has potential applications in atomic physics. If a nuclear model can

be found which consistently fits the muonic hyperfine structure, this model can be used to test electron wave functions in the calculation of hyperfine anomalies.

We have also performed calculations of hyperfine anomalies for ordinary atoms using unshielded electron wave functions.<sup>18</sup> These calcu-

lations agree moderately well with experiment only for single  $s$ -state electrons outside closed shells. In more complicated cases we obtain large deviations from experiment, including the wrong sign in some cases. Our calculations also indicate that such anomalies can only be due to  $s_{1/2}$  and  $p_{1/2}$  electrons, since the anomalies calcu-

lated for  $p_{3/2}$  states are six orders of magnitude smaller than measured values of isotopes with electrons in  $p_{3/2}$  states. The success of the muon calculations suggests that these nuclear models do satisfy Stroke's criterion, and can be used to test Hartree-Fock or configuration admixed electron wave functions.

\*Work supported in part by the National Science Foundation, first reported by J. J. at the 1969 Washington meeting of the American Physical Society, *Bull. Am. Phys. Soc.* **14**, 538 (1969).

†Work done in partial fulfillment of the requirements for the Ph.D. degree at Carnegie-Mellon University. Present address: Kenyon College, Gambier, Ohio 43022.

<sup>1</sup>F. Bitter, *Phys. Rev.* **75**, 1326 (1949).

<sup>2</sup>F. Bitter, *Phys. Rev.* **76**, 150 (1949).

<sup>3</sup>A. Bohr and V. F. Weiskopf, *Phys. Rev.* **77**, 94 (1950).

<sup>4</sup>H. H. Stroke, R. J. Blin-Stoyle, and V. Jaccarino, *Phys. Rev.* **123**, 1326 (1961).

<sup>5</sup>M. N. Suzuki, Ph.D. thesis, Carnegie-Mellon University, 1968 (unpublished).

<sup>6</sup>R. A. Carrigan, Jr., P. D. Gupta, R. B. Sutton, M. N. Suzuki, A. C. Thompson, R. E. Cote, W. V. Prestwich, A. K. Gaigalas, and S. Raboy, *Bull. Am. Phys. Soc.* **13**, 65 (1968); *Phys. Rev. Letters* **20**, 874 (1968).

<sup>7</sup>J. A. Johnson, A. C. Thompson, D. Adler, R. B. Sutton, and R. A. Sorensen, *Phys. Letters* **29B**, 420 (1969).

<sup>8</sup>R. Baader, H. Backe, R. Engfer, E. Kankeleit, W. U. Schroder, H. Walter, and K. Wien, *Phys. Letters* **27B**, 428 (1968).

<sup>9</sup>W. Y. Lee, S. Bernow, M. Y. Chen, S. C. Cheng,

D. Hitlin, J. W. Kast, E. R. Macagno, A. M. Rushton, C. S. Wu, and B. Budick, *Phys. Rev. Letters* **23**, 648 (1969).

<sup>10</sup>M. LeBellac, *Nuc. Phys.* **40**, 645 (1963).

<sup>11</sup>A. Arima and H. Horie, *Progr. Theoret. Phys. (Kyoto)* **11**, 509 (1955).

<sup>12</sup>R. J. Blin-Stoyle, *Proc. Phys. Soc., (London)* **A66**, 1158 (1953).

<sup>13</sup>J. Bardeen, L. N. Cooper, and J. R. Schrieffer, *Phys. Rev.* **108**, 1175 (1957).

<sup>14</sup>H. Noya, A. Arima, and H. Horie, *Progr. Theoret. Phys. (Kyoto) Suppl.* **8**, 33 (1958).

<sup>15</sup>L. S. Kisslinger and N. Freed, *Nucl. Phys.* **25**, 611 (1961).

<sup>16</sup>L. S. Kisslinger and R. A. Sorensen, *Rev. Mod. Phys.* **35**, 853 (1963).

<sup>17</sup>J. Johnson and R. A. Sorensen, *Phys. Letters* **26B**, 700 (1968).

<sup>18</sup>J. A. Johnson, Ph.D. thesis, Carnegie-Mellon University, 1969 (unpublished).

<sup>19</sup>S. Hinds, R. Middleton, S. H. Bjeregaard, O. Hansen, and O. Nathan, *Nucl. Phys.* **83**, 17 (1966).

<sup>20</sup>A. Covello and G. Sartoris, *Nucl. Phys.* **A93**, 481 (1967).